

https://dspace.org/

Spatial distribution of woody plants in relation to mistletoeinfected Vachellia karroo trees in a semiarid African savanna

Tsitsi Maponga; Hilton Ndagurwa; Justice Muvengwi; Edward Witkowski

https://hdl.handle.net/10539/41098
WOS

Downloaded from a DSpace repository. https://dspace.org/

Global Ecology and Conservation 51 (2024) e02931



Contents lists available at ScienceDirect

Global Ecology and Conservation

journal homepage: www.elsevier.com/locate/gecco



Original research article



Spatial distribution of woody plants in relation to mistletoe-infected *Vachellia karroo* trees in a semi-arid African savanna

Tsitsi Sithandiwe Maponga [a,b,d,1], Hilton Garikai Taambuka Ndagurwa [a,d,2], Justice Muvengwi [c,d,*,3], Ed T.F. Witkowski [a,d,4]

[a] *Department of Forest Resources and Wildlife Management/Forest Ecology Laboratory, Faculty of Applied Sciences, National University of Science & Technology, P.O. Box AC 939 Ascot, Bulawayo, Zimbabwe*
[b] *NRF/SAEON, SAEON Ndlovu Node, Private Bag X1021, Phalaborwa 1390, South Africa*
[c] *Department of Environmental Science, Bindura University of Science Education, Private Bag, 1020, Bindura, Zimbabwe*
[d] *School of Animal, Plant and Environmental Sciences, University of the Witwatersrand, Wits, Private Bag 3, Johannesburg 2050, South Africa*

ARTICLE INFO

Keywords:
Acacia
Bivariate analysis
Competitive exclusion
Facilitation
Semi-arid savannas
Univariate analysis
Vachellia karroo

ABSTRACT

By increasing resource heterogeneity, mistletoe-infected trees can restructure plant community processes and distribution patterns. No information is available on how mistletoe-infected *Vachellia (Acacia) karroo* trees within *V. karroo* dominated stands are spatially distributed, and on how they influence the spatial patterns of their surrounding conspecifics and heterospecifics. Each woody plant was stem mapped using a cartesian plane (x, y) within three 50×50 m plots located in *V. karroo* dominated stands in a semi-arid savanna, South West Zimbabwe. Pair correlations $g(r)$ were used for the univariate analysis and Poisson process null models were applied to quantify and detect overall departure from randomness. For the bivariate analysis, pair correlations $g_{12}(r)$ under the null model of independence were used, whilst the mark correlation function (kmm(r)) was used to analyse the correlation of tree canopy area and mistletoe infection intensity. For each plot, size class distributions, based on tree height and basal stem diameter displayed negative J curves, with steep negative regression slopes across the size classes, clearly indicating a strongly recruiting population of *V. karroo.* The univariate patterns of all trees (infected and non-infected) were consistent with a random pattern, which is attributed to unsystematic mistletoe seed dispersal by birds. The univariate analysis of all woody plants (adults and juveniles) exhibited aggregation at small spatial scales due to the high abundance of clustered seedlings and saplings. At small spatial scales, understory woody plants (both conspecifics and non-conspecifics) were positively associated with mistletoe-infected trees due to mistletoephily which is the facilitation (or nurse protégé interactions) within the more resource-rich mistletoe-infected tree subcanopies. These results provide strong evidence suggesting that the variations in

* Corresponding author at: Department of Environmental Science, Bindura University of Science Education, Private Bag, 1020, Bindura, Zimbabwe.
E-mail addresses: tsimap@gmail.com, 1741059@students.wits.ac.za (T.S. Maponga), hilton.ndagurwa@nust.ac.zw (H.G.T. Ndagurwa), justicemuvengwi@gmail.com (J. Muvengwi), Ed.Witkowski@wits.ac.za (E.T.F. Witkowski).
[1] ORCID: 0000-0001-9933-1915
[2] ORCID: 0000-0002-9349-6548
[3] ORCID: 0000-0002-1338-1995
[4] ORCID: 0000-0001-5453-1390

https://doi.org/10.1016/j.gecco.2024.e02931
Received 7 August 2023; Received in revised form 1 April 2024; Accepted 3 April 2024
Available online 4 April 2024
2351-9894/© 2024 The Author(s). Published by Elsevier B.V. This is an open access article under the CC BY-NC-ND license (http://creativecommons.org/licenses/by-nc-nd/4.0/).

spatial pattern modification by mistletoe-infected trees could further increase spatial heterogeneity in this semi-arid savanna. As such, by increasing heterogeneity, mistletoe-infected trees can increase the resilience of semi-arid savannas in the face of perturbations and stochastic events.

1. Introduction

In semi-arid savannas, the intricate interplay between various environmental factors such as soil heterogeneity, topography, termite mounds, and the presence of large trees profoundly influence plant diversity, structure, and community spatial patterns (Dale, 2000; Meyer et al., 2008; Rayburn, Monaco, 2011; Schleicher et al., 2011; Muvengwi et al., 2017, 2018a, 2020; Svátek et al., 2018). Among these factors, large trees, acting as keystone elements, play a pivotal role by accumulating nutrients and enhancing water availability within their subcanopies, thereby creating localized fertility islands that foster the establishment of seedlings of various woody species (Belsky, 1994; Kanz, 1996; Muvengwi et al., 2015). Consequently, the presence and spatial distribution of large trees significantly influence the composition of plant communities and the utilization of resources (Barot et al., 1999).

Mistletoe-infected trees, a common occurrence within these ecosystems, exert considerable influence on soil physical and biochemical properties due to the substantial volume of quality litter and droppings deposited within their subcanopies by birds and other animals attracted to mistletoes (Dzerefos et al., 2003; Ndagurwa et al., 2013, 2014, 2015, 2020; Mellado et al., 2016; Mellado and Zamora, 2017; Maponga, 2021). This phenomenon often leads to the facilitation of understory plants or even competitive exclusion, driven by the increased availability of resources (Maponga et al., 2021). However, while existing studies have primarily focused on the spatial patterns and distribution of mistletoes on their hosts (Overton, 1996; Aukema, 2004; Kavanagh and Burns, 2012; Sayad et al., 2017), little attention has been given to the small-scale effects of mistletoe-infected trees on the surrounding woody plants within and beyond their subcanopies.

Understanding these dynamics is crucial as mistletoes, being hemiparasitic, derive water and nutrients from their hosts while maintaining the ability to photosynthesize (Preston et al., 2010; Okubamichael et al., 2011; Arruda et al., 2012). Over time, mistletoe infection can lead to detrimental effects on the host tree, including increased transpiration rates and alterations in morphology, phenology, and physiology (Mathiasen et al., 1990; Sala et al., 2001; Bowie and Ward, 2004; Ward et al., 2006; Arruda et al., 2012; Sayad et al., 2017; Bilgili et al., 2018, 2020; Ozturk et al., 2022). These changes reduce the competitiveness of the host, thereby promoting the growth of neighbouring shrubs and trees and influencing the spatial pattern of larger size classes (Pennings and Callaway, 1996; Spasojevic and Suding, 2011; Muvengwi et al., 2015; Ndagurwa et al., 2016, 2018). Additionally, increased light incidence resulting from mistletoe infection further facilitates understory growth, particularly of sun-loving species (Mellado and Zamora, 2017; Maponga et al., 2021).

Given these ecological dynamics, spatial point pattern analysis offers a valuable tool for elucidating the scales at which specific patterns are significant and how different plant species and size classes are correlated (Fortin and Dale, 2005; Martínez et al., 2010). However, in semi-arid savannas, no known study has investigated how mistletoe-infected trees influence the spatial distribution of surrounding con- and hetero-specific woody plants of different sizes. Therefore, this study employs spatial point pattern analysis to assess the spatial distribution of mistletoe-infected *Vachellia karroo* (Hayne) Banfi & Galasso (Fabaceae) (formerly *Acacia karroo* Hayne) trees within *V. karroo* dominated stands. It is a typical spinescent, bipinnate leafed, African '*Acacia*', which is common, widespread, and indigenous to southern Africa. Specifically, we examine the spatial distribution of all woody plants, infected and uninfected *V. karroo* trees, and mistletoe-infected *V. karroo* trees, while also investigating the spatial distribution pattern of understory woody plants around mistletoe-infected *V. karroo* trees.

We expected that all woody and *V. karroo* individuals would be aggregated at small spatial scales. Infected and uninfected trees were expected to show regular distribution due to density-dependent thinning. Although large trees are expected to have a regular distribution (Ward et al., 2022), we expected that large mistletoe-infected trees would exhibit a random pattern, attributed to the bird dispersers randomly visiting amongst the largest trees. Based on the host quality hypothesis this suggests that dispersers and mistletoes would target and be compatible (respectively) with hosts with the highest benefits for their productivity (Dean et al., 1994; Kolodziejek and Kolodziejek, 2013; Mellado and Zamora, 2017; Ndagurwa et al., 2012; Okubamichael et al., 2011, 2014; Overton, 1996; Press and Phoenix, 2005; Roxburgh and Nicolson, 2005, 2008; Daryaei and Moghadam, 2012; Pinto, 2005). Lastly, we expected a positive association between mistletoe-infected trees and specific understory woody plant species, known as mistletoephily (Maponga et al., 2021). We assumed that mistletoe-infected tree subcanopies would be 'safe sites' for a diversity of plant species being nursed by the mistletoe host tree. However, due to augmented nutrients and possible soil moisture limitation, facilitation is expected for the most resource competitive species within the safe sites. Through this comprehensive analysis, we aimed to provide insights into the complex interactions between mistletoe-infected trees and surrounding woody plant species, shedding light on their spatial dynamics and ecological implications in semi-arid savanna ecosystems.

2. Methodology

2.1. Study area

The study was carried out at the 28 000 ha Matopos Research Station (MRS) South West Zimbabwe (20° 31'S, 28° 31'E, 1340 m a.s.l.), 30 km south west of Bulawayo (Chirara et al., 1998; Moyo et al., 2011; Mupangwa et al., 2013). MRS is an agricultural research

station that was established in 1903. It is fenced and has free ranging livestock e.g., cows', goats, and sheep that graze throughout the year. The area is very dry and has a recommended stocking rate of 1 livestock unit per 10 ha (Ovincent et al., 1960). There have not been any recent instances of vegetation fire, but trees are occasionally harvested for firewood. MRS receives mean annual precipitation of 586 mm whilst the mean annual temperature is 18 ºC. The soils are predominantly medium-textured schist-derived siallitic red clay soils of moderately high fertility (Dye, 1983). These fine-textured soils are dominated by *V. karroo* trees that are indigenous to southern Africa. Nonetheless, MRS is generally dominated by a homogenous thornveld consisting mostly of several *Vachellia* (*Acacia*) species (*V. karroo, V. nilotica* subsp. *kraussiana, Vachellia gerrardii* (Benth.) P.J.H. Hurter, and *Vachellia rehmanniana* (Schinz) Kyal. & Boatwr.). At MRS, *V. karroo* is one of the main hosts of mistletoes such as *Viscum verrucosum* Harv (Viscaceae), *Plicosepalus kalachariensis* (Schinz) Danser (Loranthaceae), and *Erianthemum ngamicum* (Sprague) Danser (Loranthaceae) (Ndagurwa and Dube, 2013; Ndagurwa et al., 2013, 2016). It must be noted that our study tree, *Vachellia karroo,* formerly *Acacia karroo* Hayne, was reclassified in 2011 at the 17th International Botanical Congress in Melbourne (Dyer, 2014). African Acacias were split into two genera (*i.e., Vachellia* and *Senegalia*) based on their morphological, anatomical, and biochemical characteristics (Dyer, 2014).

2.1.1. Woody species mapping and measurements

Sampling was carried out between March and April 2018. Three relatively homogenous (with little differences in physical environmental characteristics (very flat slope) or level of herbivory) 50 × 50 m (0.25 ha) plots were randomly selected within *V. karroo*-dominated areas. These plots were located within a 1 km radius of each other; with little if any environmental differences between plots. In each of the three plots, all the large, mature trees were *V. karroo*, although there were numerous smaller sized woody plants of other species as well. The location of every woody plant was stem-mapped (*x*–*y* coordinates) on a Cartesian plane. The Cartesian plane specifies each point uniquely in space by a pair of numerical coordinates, i.e., distances to the point from two fixed perpendicular directed lines (Dale, 2000; Pillay and Ward, 2012). The plots were subdivided into ten, 5 × 50 m transects to ensure the accuracy of the coordinates. For trees with a single stem base, the coordinates of the stem base were taken whilst, for multi-stemmed plants, the canopy centroid coordinates were recorded. For each woody plant, the species and its size (height, stem diameter, long and perpendicular crown diameter (D_1 and D_2), canopy area ($\pi(D_1/2)(D_2/2)$), and number of mistletoes/tree were recorded. Individual woody plants were classified using stem diameter into four-stage classes, seedlings (stem diameter, ≤ 0.19 cm), saplings (stem diameter, ≥ 0.20 cm), shrubs (stem diameter $\geq 1.01 \leq 4$ cm), and trees (stem diameter, ≥ 4 cm).

2.2. Data analysis

2.2.1. Univariate analysis

To detect density-dependent competition between neighbouring mistletoe-infected trees resulting from second-order effects in the plots, the nearest neighbour analysis was used (Muvengwi et al., 2018b). Second-order effects are those effects that result from the interaction of spatial points of the pattern. The nearest neighbour analysis estimates the likelihood of finding the nearest mistletoe-infected tree within a distance *r* of the representative mistletoe-infected tree in each plot. It was calculated using the package *spatstat* and the nearest neighbour function *gest*. All univariate and bivariate analyses were conducted in the r environment (R Core Team, 2020)

Univariate distribution within each plot of (1) all the different woody plant individuals, (2) all stages of *V. karroo* individuals only, (3) mistletoe-infected *V. karroo* trees, (4) all the large, mature *V. karroo* trees (inclusive of mistletoe-infected trees) was analysed using the pair correlation *g*(*r*) function from the *spatstat package.* The small-scale point pattern of mapped trees was analysed using the pair correlation function *g*(*r*).

The pair correlation function uses standardised density to describe patterns (Getzin et al., 2006, 2011) and it is non-cumulative, provides better interpretation of neighbourhood density and can detect specific distances wherein there are violations to the null hypothesis (Velázquez et al., 2014; Muvengwi et al., 2018b). Furthermore, the pair correlation uses the probability density function which is intuitive in evaluating scale-dependent effects. Consequently, the pair correlation function does not muddle effects at shorter, compared with those at longer distances, thus revealing the different scales of a pattern at all distances (Moustakas et al., 2008; Muvengwi et al., 2018a). Detecting varying patterns across broad scales is critical in defining processes that occur at different spatial scales in any ecological system (Wiegand et al., 2007). The pair correlation approximates the probability of discovering a tree at distance *r* from a representative focal point, normalized by dividing by the intensity (λ) of the pattern (Dohn et al., 2017). Therefore, *g*(*r*) details the spatial structure i.e., aggregation and regularity at known radius *r* based on inter tree distances:

$$g(r) = \frac{K'(r)}{2\pi r} \quad for \geq 0 \tag{1}$$

For all the point pattern analyses, Ripley's isotropic correction which accounts for edge effects was applied. Furthermore, we also considered the occurrence of homogeneity in the point patterns of each plot to select the appropriate null model. For plots with heterogeneous patterns, the heterogeneous Poisson process null model was applied, whilst, for plots with homogeneous patterns, the null model of CSR (homogeneous Poisson process) was applied to quantify and detect overall departure from randomness (Velázquez et al., 2014; Ben-Said, 2021; Getzin et al., 2011). The heterogeneous Poisson process null model takes into account environmental heterogeneity effects and eliminates aggregation which can be influenced by first-order heterogeneity (Ben-Said, 2021). In addition, to determine if there is a significant difference between the actual observed pattern and the null model, all the summary statistics (univariate pattern analyses) were assessed using 199 Monte Carlo simulations (5th lowest and 5th highest value). These generated

95% simulation envelopes, from which assessment of departure of the observed pattern from the null model was quantified (Baddeley et al., 2014, 2015). Furthermore, the Diggle-Cressie-Loosmore-Ford test (DCLF) was used to investigate whether the observed spatial patterns were significantly different from the null hypothesis of complete spatial randomness since simulation envelopes are susceptible to Type 1 error (Velázquez et al., 2014; Baddeley et al., 2014; Dohn et al., 2017; Ward et al., 2022).

2.2.2. Bivariate analysis

For bivariate analysis, data was split into sub-patterns of mistletoe-infected trees and understory woody plants (seedlings, saplings and shrubs combined). The bivariate point-pattern analyses the pattern between two species of plants or two stage classes of the same species, on whether their distribution is independent of each other (Dale, 2000; Wiegand and Moloney, 2013). The patterns of interaction between mistletoe-infected trees and understory woody plants were tested using bivariate statistics i.e., bivariate estimator for pair correlation, $g_{12}(r)$ function:

$$g_{12}(r) = \frac{K'_{12}(r)}{2\pi r} \tag{2}$$

Furthermore, when there are two types of points representing sub-populations (which are/not interacting), the null hypothesis of independent labelling is most appropriate (Baddeley et al., 2015). Thus, the null model of independence was used to investigate whether the understory woody plants were facilitated or inhibited by mistletoe-infected *V. karroo* trees. This model assumes that two independent processes are responsible for generating the mistletoe-infected tree and the understory woody plant patterns (Wiegand and Moloney, 2004; Ben-Said, 2021). Under independent labelling, understory woody plants in an originally non-marked point process are *a posteriori* independently marked while keeping the locations and labels of mistletoe-infected trees fixed (Svátek et al., 2018). Using the arguments rshift and radius = 150 (which selects a random point in the disc radius 150) we tested the independence of components hypothesis, and the sub-patterns were randomly shifted independently of each other (Baddeley et al., 2015). A bivariate pair correlation function $g_{1,2}(r)$ above or below the simulation envelopes indicates that there are more (attraction) or fewer understory woody plants (repulsion) around mistletoe-infected than under independent labelling, respectively (Wiegand and Moloney, 2004; De La Cruz et al., 2008; Svátek et al., 2018). If the null hypothesis of independence is not rejected, this suggests that components are independent (Baddeley et al., 2015).

2.2.3. Mark correlation function

The mark correlation function $k_{mm}(r)$ for quantitative marked patterns was used to investigate if canopy area or mistletoe counts on pairs of infected trees exhibited any spatial correlation dependent on their distance r. The relationship between the mistletoe-infected trees and their characteristics (canopy area, mistletoe numbers) was quantified for positive real-value marks, as f (m, m′) = mm′, (Baddeley et al., 2015). There were three possible outcomes of the relationship between the marks, i.e., if m × m′ of canopy area or mistletoe numbers of two trees separated by distance r were equal to the overall marks mean μ, i.e., if $k_{mm}(r) = 1$, then there is no spatial correlation, if $k_{mm}(r) > 1$, there is a positive association (correlation), and lastly, if $k_{mm}(r) < 1$ there is a negative association (Muvengwi et al., 2018a). Departure from independent marking null model, which randomly shuffles the marks (canopy area or mistletoe counts) between pairs of trees, was evaluated using the 5th lowest and 5th highest values of 199 Monte Carlo simulations to generate ~99% simulation envelopes (Baddeley et al., 2014).

3. Results

3.1. Structural attributes, density, species richness and mistletoes/tree

The total number of woody plants and stand density was highest in plot 2 and lowest in plot 1 (Table 1). Seventeen woody species were observed across the three plots (Appendix 1). Plot 3 had the lowest species richness, whilst plot 2 had the highest, with *V. karroo* being the dominant species for plot 1 (87%) and plot 2 (74%), but not plot 3 (23%), which was dominated by smaller stage classes of *Ziziphus mucronata* Willd. subsp. *mucronata* (Rhamnaceae) (49.1%), (Appendix 1). All the plots were dominated by saplings, with relative abundances from 74% to 80% (Appendix 2). Stem diameter and height across the plots ranged from 0.10 to 46 cm and 0.02–10.30 m (Table 1). All mature trees recorded in this study were *V. karroo*.

There were negative J shaped size class distributions (SCD) curves of *V. karroo* for height and stem diameter in each plot (Fig. 1). All

Table 1
Number of woody plants, stand density/ha, number of woody species, stem diameter and height ranges/plot in the three plots. SE – standard error.

Parameter	Plot number			
	Plot 1	Plot 2	Plot 3	Mean ± SE
Total woody plants	1100	2174	1273	1515 ± 333
Stand density/ha	4400	8588	5092	6027 ± 1296
Number of woody species	11	13	10	11.33 ± 0.88
Stem diameter range/plot (cm)	0.10–34.00	0.10–46.00	0.10–31.2	
Height range/plot (m)	0.3–8.20	0.02–8.50	0.02–10.30	

SCDs had negative slopes, indicating a strongly recruiting *V. karroo* population (Table 2), attributed to large numbers of smaller compared to larger sized plants. Further, the relationship between height and stem diameter of *V. karroo* individuals and different stage classes in all three plots showed a positive relationship (Fig. 2).

The number and density of mistletoe-infected trees was generally higher in plot 3 and lowest in plot 1 (Table 3). There was a significant difference in the stem diameter (Kruskal Wallis $\chi^2 = 9.33$, $df = 2$, $P = 0.01$), canopy area (Kruskal Wallis $\chi^2 = 7.03$, $df = 2$, $P = 0.03$) and mistletoes/tree counts (Kruskal Wallis $\chi^2 = 8.42$, $df = 2$, $P = 0.01$) on mistletoe-infected *V. karroo* trees across the three plots (Table 3), but no differences in tree height (Kruskal Wallis $\chi^2 = 0.35$, $df = 2$, $P = 0.83$).

V. verrucosum was by far the most dominant mistletoe species (94.6% of individuals), occurring on all infected *V. karroo* trees except for one in plot 3. The other two species were less prevalent, namely *P. kalachariensis* (5.1%), and *E. ngamicum* (0.3%) (Table 3). Uninfected mature trees tended to be smaller in height and DBH than mistletoe-infected mature trees (Fig. 3).

3.2. Univariate analysis

Plot 1 (5.77 ± 0.52 m) had the longest mean nearest neighbour distance, whilst both plot 2 (3.84 ± 0.33 m) and plot 3 (3.68 ± 0.16 m) had much shorter nearest neighbour distances.

The univariate analysis of all the woody species in each of the three plots showed strong evidence of aggregation ($g(r)>1$) (DCLF test: $P < 0.05$, Table 4) at distances from 0.5 to 1 m, 0–7.2 m, and 0.2–1.4 m for plot 1 to plot 3, respectively (Fig. 4a-c). At greater distances, each of the three plots had a random pattern (Fig. 4).

Similarly, the spatial pattern ($g(r)$) for all the *V. karroo* individuals (Fig. 4d-f) confirmed significant aggregation at distances from 0.5 to 0.75 m, 0–1.8 m, and 0.2–1 m for plot 1 to plot 3, respectively (DCLF test: $P < 0.05$, Table 4). However, (i) mistletoe-infected trees and (ii) all the trees showed a completely random pattern ($g(r) = 1$) across the three plots (Fig. 4 g-i and Appendix 3, respectively, DCLF test: $P > 0.05$, Table 4).

3.3. Bivariate analysis

Understory woody plants were positively associated with mistletoe-infected trees at distances from 1 to 1.5 m and 0–1 m in plot 2 and plot 3, respectively, whilst plot 1 showed no association (Fig. 5a-c). Further, all understory plants were negatively associated with mistletoe-infected trees at distances from 2 to 3 m and 7–7.2 m in plot 2 and plot 3, respectively.

3.4. Mark correlation

The univariate mark correlation function in plot 1 showed that canopy areas of mistletoe-infected trees at shorter distances were larger than those further away from each other (Fig. 6a). However, overall mistletoe-infected tree canopy areas in plot 1 showed independence at all the distances. In contrast, in plot 2 and plot 3, the canopy areas of two nearby mistletoe-infected trees were smaller than pairs situated farther away from each other (Fig. 6b-c). Furthermore, there was a significant negative correlation at distances between 1 and 3 m for both plot 2 and plot 3 signifying presence of competition at shorter distances (Fig. 6b-c).

Likewise, the number of mistletoes found on mistletoe-infected trees at shorter distances apart tended to be more than found at

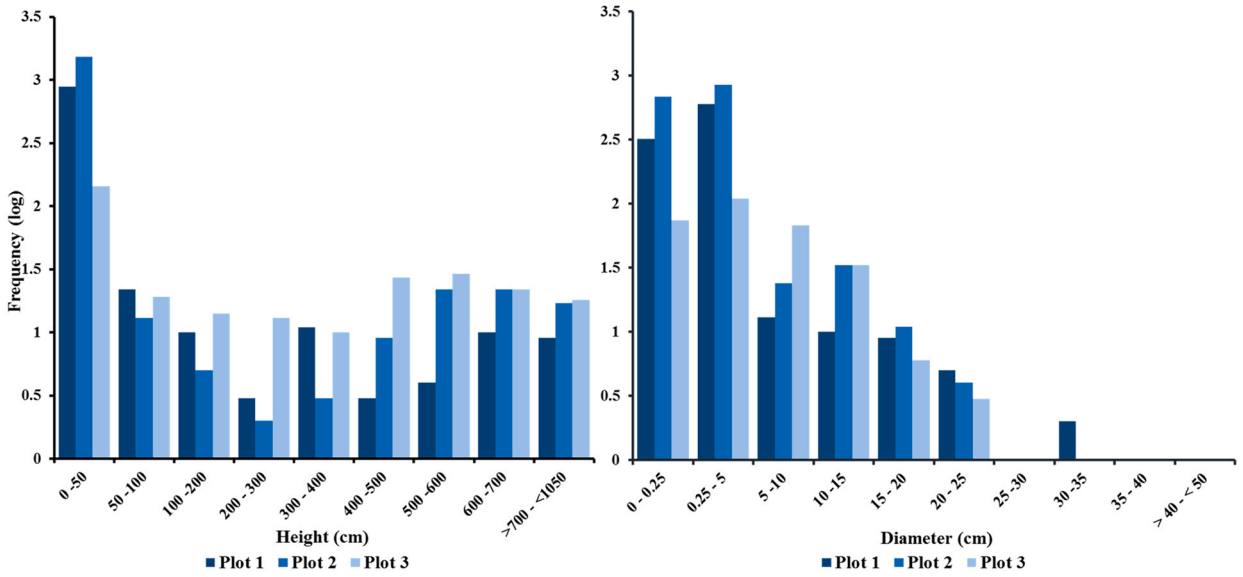

Fig. 1. Frequency ($\log_{10}$) of *Vachellia karroo* individuals in each height and diameter size class for plots 1–3.

Table 2
Summary table of the slope of regression (height *vs*. number of individuals, diameter at breast height (dbh) *vs*. number of individuals).

Variable	SCD slope (°)	r^2	*t*	*P*
Height				
Plot 1	-0.69	0.68	-3.81	0.01
Plot 2	-0.72	0.57	-3.07	0.02
Plot 3	-0.37	0.64	-3.50	0.01
All plots	-0.77	0.65	-3.58	0.01
Diameter				
Plot 1	-0.95	0.95	-12.73	<0.001
Plot 2	-0.99	0.97	-15.97	<0.001
Plot 3	-0.84	0.99	-12.15	<0.001
All plots	-1.0	0.99	-16.00	<0.001

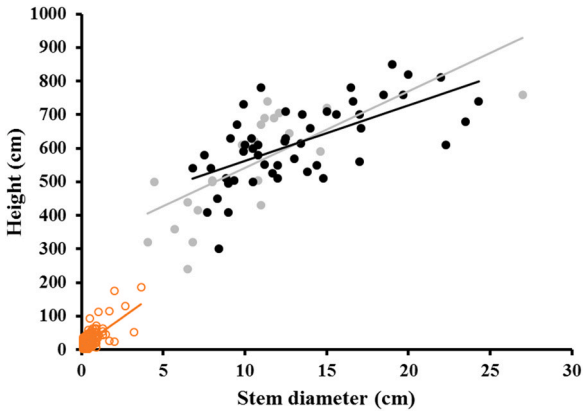

Fig. 2. Relationship between stem diameter (cm) and height (cm) of all *Vachellia karroo* trees recorded in the three plots combined but according to size classes, i.e., orange open dots show seedlings, saplings, and shrubs, respectively, while grey and black closed dots represent uninfected and infected *V. karroo* mature trees, respectively. Regression lines for mistletoe-infected trees (black, $r^2 = 0.41$), uninfected trees (grey, $r^2 = 0.51$), and orange (for immature plants, i.e., seedlings, saplings, and shrubs, $r^2 = 0.41$) are shown.

Table 3
Number and density of all large, mature *Vachellia karroo* trees (mistletoe-infected and uninfected trees), their stem diameter, height, canopy area, density, proportion and mistletoes/tree (mean ± S.E, and range), total number of mistletoes/plot, and numbers of the three mistletoe species/plot. Means in rows not sharing a small common letter are significantly different (Kruskalmc, $P < 0.05$).

Parameter	Plot number		
	Plot 1	Plot 2	Plot 3
Overall tree attributes			
Total number of trees/plot	42	77	120
Density of trees/ha	168	308	480
Stem diameter/plot (cm)	15.76 ± 1.40^{a}	13.85 ± 0.89^{ab}	11.80 ± 0.67^{b}
Height/plot (m)	5.67 ± 0.37^{a}	6.20 ± 1.67^{a}	6.18 ± 0.22^{a}
Canopy area/plot (m^2)	28.11 ± 3.42^{a}	21.06 ± 2.19^{ab}	18.76 ± 1.80^{b}
Mistletoe infected tree attributes			
Number of mistletoe-infected trees/plot	32	52	61
Density of mistletoe-infected trees/ha	128	208	244
Proportion of infected trees (%) from the total number of trees	76%	68%	51%
Number of mistletoes/infected tree	3.21 ± 0.42^{b}	5.37 ± 0.76^{a}	4.12 ± 0.72^{ab}
Number of mistletoes/infected tree (range)	1–9	1–25	1–31
Total number of mistletoes	222	275	247
Number of *Viscum verrucosum* (number of trees infected)	212 (32)	263 (52)	229 (60)
Number of *Plicosepalus kalachariensis* (number of trees infected)	8 (4)	12 (9)	18 (27)
Number of *Erianthemum ngamicum* (number of trees infected)	2 (2)	0 (0)	0 (0)

greater distances apart in plot 1 (Fig. 6d). However, in plot 2, the number of mistletoes on two nearby trees was negatively correlated ($P < 0.05$) at distances between 1 and 2.8 m (Fig. 6e). Plot 3 showed independence at distances from 0 to 6.8 m before showing a marginal positive correlation at distances around 7 m apart (Fig. 6f).

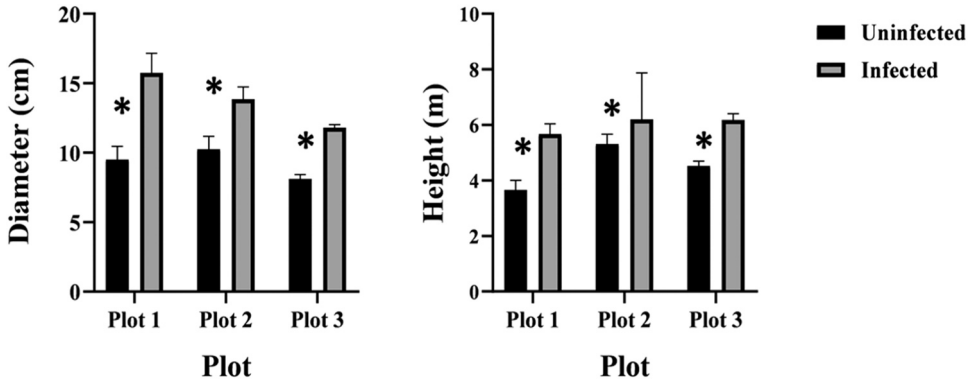

Fig. 3. Comparison (mean ± standard error) of a) stem diameter and b) height of mistletoe-infected and uninfected trees (all *Vachellia karroo*) within each plot (1–3, with decreasing proportions of infected *V. karroo* trees). Asterisks show differences between mistletoe-infected and uninfected trees per plot ($P < 0.05$).

Table 4
Results of the Diggle-Cressie-Loosmore-Ford Test (DCLF) of complete spatial randomness under Monte Carlo, based on 199 simulations with fixed number of points.

	Plot number	u-value	*P*	Rank
All woody species	1	4.56	**0.01**	1
All woody species	2	6.28	**0.01**	1
All woody species	3	2.27	**0.01**	1
V. karroo only	1	4.05	**0.01**	1
V. karroo only	2	5.34	**0.01**	1
V. karroo only	3	3.90	**0.01**	1
V. karroo with mistletoes	1	21.33	0.09	9
V. karroo with mistletoes	2	0.50	0.94	188
V. karroo with mistletoes	3	1.46	0.58	115
All trees	1	3.68	0.30	61
All trees	2	4.91	0.12	12
All trees	3	0.53	0.74	74

4. Discussion

The three randomly chosen plots had considerable differences in total woody plant density, as well as understorey species composition, which was predominately made up of saplings. In agreement, the regression slopes were negative across the size classes, showing a strongly recruiting population of *V. karroo*. There was only a single mistletoe host tree species, *Vachellia karroo*, which also differed in density between the three plots. As such, plot 1 had the lowest number and density of all large mature trees and mistletoe-infected trees compared to plot 3, which had the highest. However, stem diameter and canopy area were larger in plot 1 and smaller in plot 3. Plot 2 had the highest number of mistletoes/infected tree, while plot 1 had the least. Nonetheless, there was little variation in the heights of all the large, mature trees between the plots. Mistletoe-infected trees were taller and had larger stem diameters than uninfected trees across the plots. In the context of these and other similarities and differences between the plots, the main findings of the study are that (a) the univariate patterns for all the woody species and all the *V. karroo* individuals within each plot were consistent with aggregation at shorter scales and a random pattern at larger scales. Higher subcanopy relative to inter canopy soil resources, enhanced reproductive capacities, and changes in light incidence beneath mistletoe-infected and uninfected adult *V. karroo* trees can cause this observed small-scale aggregation. (b) Mistletoe-infected trees showed a univariate random distribution, as did all trees (infected and uninfected trees combined). This type of pattern is frequently related to the coexistence of aggregation and dispersion in several areas within these relatively large plots. (c) Lastly, there was a positive association (especially in plot 2 and plot 3) of understory woody plants with mistletoe-infected trees, indicating mistletoephily (Maponga et al., 2021), a phenomenon supported by augmented resources beneath mistletoe-infected tree canopies. In the following, we discuss the possible causes of the observed patterns and whether the resulting patterns are consistent with our projected hypothesis.

All the large, mature trees (inclusive of mistletoe-infected trees) were randomly distributed across the three plots, contrary to the regular pattern that we had initially predicted. We had expected that as trees grow, space and resource limitations would increase, leading to competitive exclusion and density-dependent mortality (Schleicher et al., 2011; Pillay and Ward, 2012; Cheng et al., 2014; Pablo and Gusman, 2017; Muvengwi et al., 2018a; Ward et al., 2022) and thus a negative spatial association would become more pronounced (Phillips and MacMahon, 1981; Barot et al., 1999; Meyer et al., 2008; Gary and He, 2009; Velázquez et al., 2014; Ward et al., 2022). However, the random pattern could be due to presence of both positive and negative associations in different areas within each of the plots, depending on the competitive abilities of neighbouring trees. Some portions of the plots had larger trees with smaller

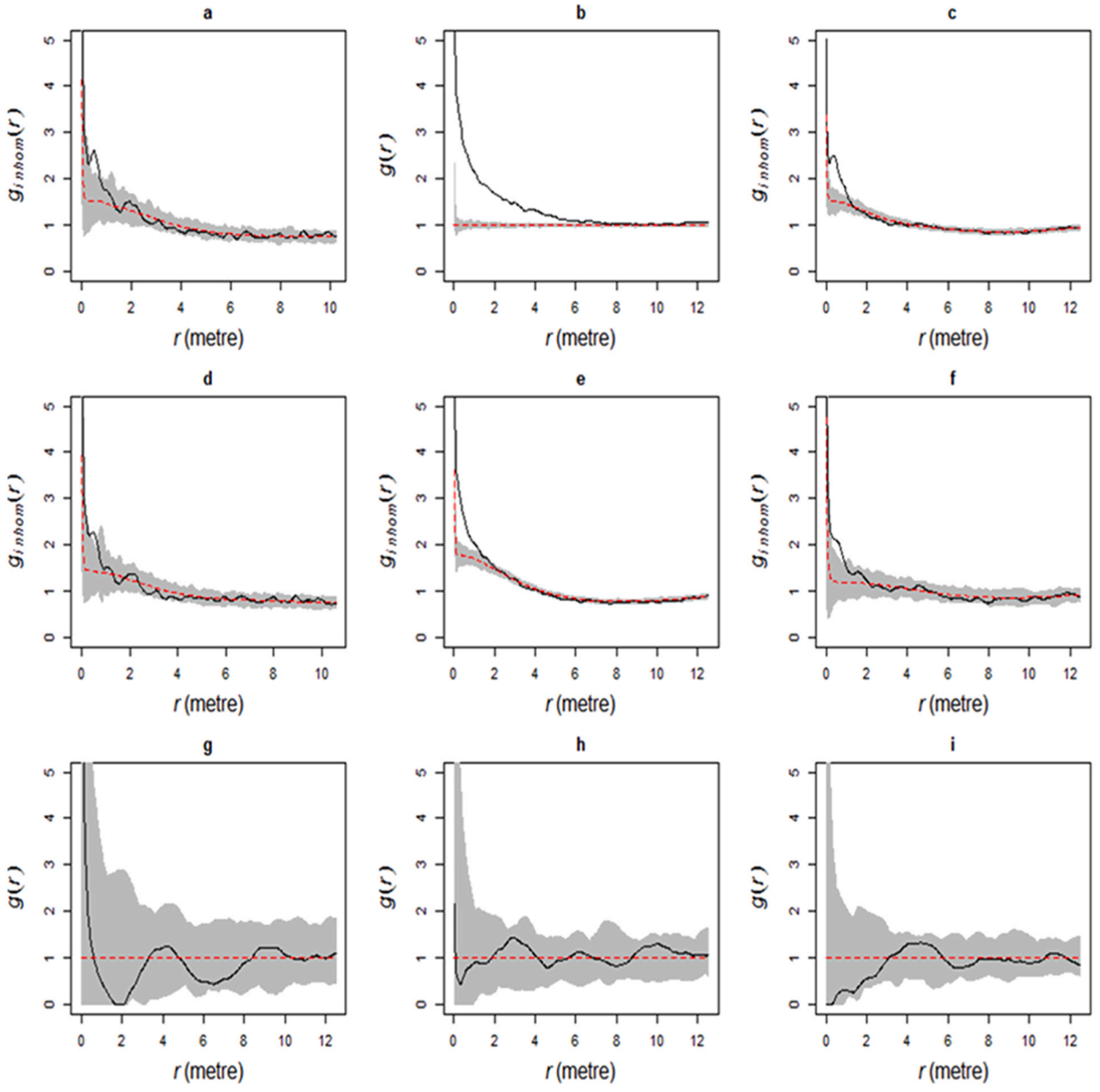

Fig. 4. Summary of univariate analysis showing the spatial patterns of all woody plants occurring in each plot (a-c), all the *Vachellia karroo* trees only (d-f), and mistletoe-infected *V. karroo* trees (g-i) within the three plots (1–3 respectively, with decreasing proportions of infected *V. karroo* trees), using the pair correlation function $g(r)$. The grey shaded areas show the upper and lower critical boundaries of the 95% point-wise envelopes, i.e., the 5th lowest and 5th highest values of the pair correlation function (g) estimated from 199 Monte Carlo simulations with either the heterogeneous Poisson or homogeneous null model of CSR (black lines). If the black line is above, below and within the grey area, then the pattern is clustered, regular or random, respectively.

tree neighbours such that even if competition was present, mortality had not (yet) been induced, thus leading to aggregation. Whereas other parts of the same plots had predominantly large neighbouring trees which are able to disproportionately acquire resources, thus resulting in density-dependent thinning, leading to a regular pattern (Meyer et al., 2008; Wiegand et al., 2008; Gary and He, 2009; Pillay and Ward, 2012; Dohn et al., 2017).

The univariate pattern and the mark correlation function of mistletoe-infected trees were predominantly consistent with a random pattern in all three plots, supporting our initial hypothesis. Although the results showed that mistletoe-infected trees could have as many as 25–31 mistletoes/tree (indicating considerable within-tree mistletoe dispersal), this individual tree mistletoe infection intensity, did not translate to mistletoe-infected trees exhibiting a clustered pattern. Therefore, the random distribution of mistletoe-infected trees could relate to the mistletoes inability to occupy all suitable habitats (mature *V. karroo* trees), dispersal limitations

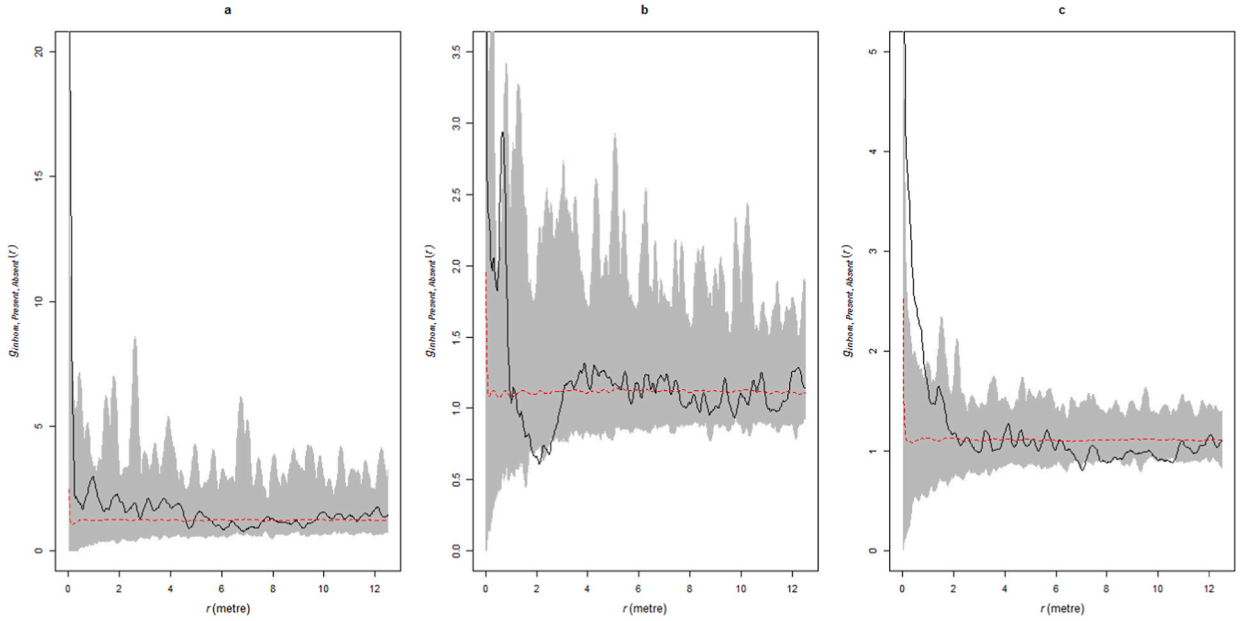

Fig. 5. Summary statistics of bivariate $g_{12}(r)$ patterns of mistletoe-infected trees with all understory plants for plot 1 to plot 3 respectively (a-c) (with decreasing proportions of infected *V. karroo* trees). The null model of independence was used, and the grey shaded areas show the upper and lower critical boundaries of the 95% point-wise envelopes i.e., the 5th lowest and 5th highest values of the pair correlation function estimated from 199 Monte Carlo simulations (black lines). The position of the black line across the scale, determines the pattern, if it is either below or above the simulation envelopes this indicates that there are fewer or more understory plants around mistletoe-infected trees than under independent labelling, respectively. Note different Y-axis scales.

that prevent efficient and effective mistletoe seed dispersal, poor host quality, or historical recruitment events of *V. karroo* before they were infected by mistletoes (Overton, 1996; Sayad et al., 2017). The random pattern exhibited by mistletoe-infected trees could also be influenced by disperser preferences and the interaction of mistletoes with dispersers, which may not necessarily be systematic (Overton, 1996; Aukema, 2004; Okubamichael et al., 2011, 2011b; Kavanagh and Burns, 2012; Sayad et al., 2017). Bird dispersers prefer to perch, feed, and build nests on taller trees with larger canopies and greater food resources (Okubamichael et al., 2014; Sayad et al., 2017), and thus they could have randomly selected trees with these characteristics. Likewise, mistletoes survive at higher rates on older, taller, and larger trees because these hosts are a reliable source of nutrients and water, even throughout the dry season (Ndagurwa et al., 2012; Okubamichael et al., 2014; Sayad et al., 2017).

Despite the overall random patterns of mistletoe-infected trees across the three plots, some important differences were observed. The mean plot nearest neighbour distances varied from 3.6 to 5 m depending on the density of mistletoe-infected trees within the plots. Subsequently, the characteristics of mistletoe-infected trees also differed between plots. This could have caused the disparities of other spatial patterns observed between plots. For instance, an increase in the density of mistletoe-infected trees (plot 2 and plot 3), suggests weak competition for resources within these plots. Therefore, mistletoe-infected trees in plot 2 and plot 3 could have invested in height growth rather than in extending their canopies; a typical response to density-dependent thinning, thus, the overall pattern tends towards aggregation (Gary and He, 2009). Further, the number of mistletoes/tree was highest in plot 2, which could have augmented nutrients from the mistletoe and animal litter deposits (Ndagurwa et al., 2014), thus further supporting the presence of mistletoephily and the competitive growth of subordinate trees/shrubs within this stand (Maponga et al., 2021). In contrast, mistletoe-infected trees in plot 1 had larger canopy areas, which could result in greater competition, thereby driving the pattern towards regularity, as shown by their lower density. Further, similar to other studies (Kolodziejek and Kolodziejek, 2013; Bilgili et al., 2020a), which report that high density tree stands have lower mistletoe prevalence, plot 1, which had the fewest trees, had the highest proportion of mistletoe-infected trees. This is despite having the lowest total number of mistletoes and number of mistletoes/tree. These differences could indirectly be a baseline for predicting potential scenarios most likely to occur at different mistletoe-infected tree densities.

In agreement with our expectations, mistletoe-infected trees facilitated positive plant interactions with understory woody plants, particularly in plot 2 and plot 3. Saplings dominated all the plots, and their high relative abundances could have influenced the small-scale clustering patterns that were observed within the plots (Ward et al., 2022). However, mistletoe-infected tree subcanopy microsites could have supported nurse protégé interactions due to augmented resources (Ndagurwa et al., 2013, 2014, 2015, 2020; Mellado et al., 2016; Mellado and Zamora, 2017), resulting in coexistence and survival of heterospecific seedlings and their recruitment into saplings. Furthermore, enhanced soil moisture in the subcanopy of mistletoe-infected trees could have increased the establishment of seedlings and the survival of saplings (Wilson and Witkowski, 1998; Maponga, 2021). This positive spatial relationship between different species and understory plants growing close to large trees is common in semi-arid savannas and may explain why there were more than 10 different species in each plot (Meyer et al., 2008; Schleicher et al., 2011; Pillay and Ward, 2012; Dohn

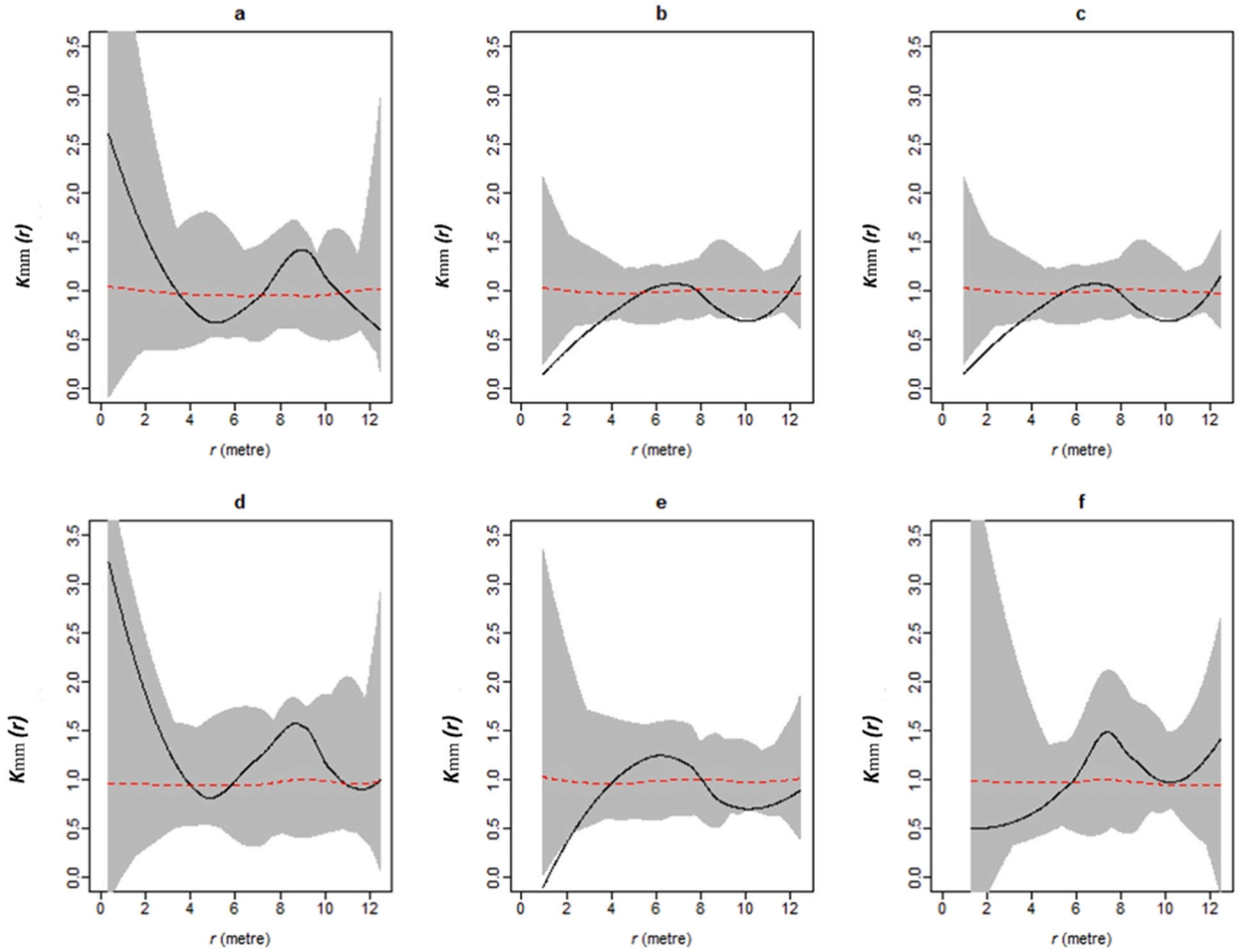

Fig. 6. Summary of the mark correlation function $k_{mm}(r)$, within the three plots (1–3; with decreasing proportions of infected *V. karroo* trees), for canopy area (a-c), and number of mistletoes per tree (d-f). Grey-shaded areas shows the envelopes (5th highest and 5th lowest values) constructed using 199 Monte Carlo simulations. The mistletoe-infected trees are either positively or negatively correlated if the black line is above or below the grey-shaded envelopes.

et al., 2017). Moreover, trees such as *Ziziphus mucronata* and *Flueggea virosa* (Roxb.ex Willd.) Voigt (Phyllanthaceae) which have a significant presence in high-resource mistletoe-infection tree subcanopies (Maponga et al., 2021), were also recorded in this study. Therefore, clustering of these small stage classes combined at shorter distances, suggests their affinity to infected tree subcanopies i.e., mistletoephily, consequently making mistletoe-infected tree subcanopies, 'safe sites', which facilitate successful germination and recruitment of a variety of seedlings and saplings (Maponga et al., 2021).

High seedling recruitment from accumulated seeds beneath mistletoe-infected trees (Flores and Jurado, 2003; Schleicher et al., 2011; Dohn et al., 2017; Mellado and Zamora, 2017, Maponga, 2021), vegetative reproduction, directed seed dispersal, and increased germination underneath mistletoe-infected trees, could also have led to the aggregation of *V. karroo* seedlings and saplings (Phillips and MacMahon, 1981; Barot et al., 1999; Witkowski and Garner, 2000; Walters and Milton, 2003; Getzin et al., 2006; Schleicher et al., 2011; Cheng et al., 2014; Maponga et al., 2021; Ward et al., 2022). This could also be the same reason, why from the univariate analysis there was significant clustering of all *V. karroo* individuals across the three plots. Indeed, other studies have also reported clustering as the overall univariate spatial pattern of *Vachellias* (formerly *Acacias*) and other woody species (Meyer et al., 2008; Pillay and Ward, 2012). Therefore, the presence of both uninfected and mistletoe-infected *V. karroo* trees results in high-resource subcanopies, which could have promoted the facilitation and recruitment of a variety of understory woody plants (Barot et al., 1999; Dale, 2000; Meyer et al., 2008; Rayburn, Monaco, 2011; Schleicher et al., 2011; Velázquez et al., 2014; Tamjidi and Lutz, 2020; Maponga et al., 2021; Maponga, 2021).

The diversity of tree species and aggregation of smaller stage classes in clumps could also have been influenced by the variation in shading. Shade-intolerant species could have colonized and aggregated within areas with higher light and temperature conditions (Mellado et al., 2017; Maponga et al., 2021), attributed to reduced foliar cover of the mistletoe-infected, compared to uninfected, trees (Bilgili et al., 2018, 2020; Ozturk et al., 2022). In contrast, areas directly underneath the mistletoe clumps (composed of leaves, fruits, flowers, and many branches) that are completely shaded could have also favoured the establishment of more shade-tolerant species

thus further leading to aggregation. For example, *V. karroo* trees are facultative sciophytes (heliophytes that can also grow under shade); hence *V. karroo* seedlings and saplings may occur in higher densities at short distances around the mistletoe-infected tree (O'Connor, 1995; Maponga, 2021).

Lastly, the effects of mistletoe-infected trees go beyond plant community structure; they also influence animal movements in semi-arid environments. A variety of animals, including birds and livestock, tend to be attracted to both mistletoe-infected tree canopies and canopy patches due to mistletoes, which flower a couple of times a year, and the diverse understory plants (attributed to high litter volume and decomposition rates). In turn, these animals also deposit excreta, further increasing nutrient availability within these mistletoe-infected tree canopy patches (Ndagurwa et al., 2013; Mellado et al., 2016; Watson, 2016; Maponga, 2021). Therefore, in the face of erratic rainfall and high temperatures, woodlands with mistletoe-infected trees are crucial as they are nutrient hotspots for both plants and animals, and they may help buffer climate change impacts in semi-arid savannas.

5. Conclusion

This study provides insight into the woody plant distribution patterns as influenced by mistletoe-infected *V. karroo* trees in a semi-arid savanna system. Mistletoe-infected trees were randomly distributed, possibly due to seed-disperser-bird preferences and the already existing random patterns of large trees common in the savanna. The random pattern displayed by infected and uninfected trees can be due to the presence of both negative (from strong competition) and positive associations (from promotion of growth due to weak competition and increased availability of resources). However, understory woody plants were positively associated with mistletoe-infected trees, probably due to facilitation (via increased nutrients and/or the weak competitive ability of the disease-ridden host), variations in light intensity underneath the tree canopies attributed to mistletoe-infected tree's foliar loss (increasing light incidence) and augmented light inhibition due to mistletoe-clumps (decreased light incidence). Of interest, the three plots displayed varying spatial patterns which was attributed to the differences in the mistletoe-infected tree densities. Therefore, these inconsistencies in spatial pattern modification by mistletoes increases spatial heterogeneity in this semi-arid savanna.

Moreover, mistletoe-infected trees will eventually die creating gaps for the establishment and survival of the subdominant heterospecific tree species. Despite our results showing a strongly recruiting *V. karroo* population, presence of subdominant heterospecific woody species will likely result in a more mixed woodland with higher species richness and diversity. Together, these results strongly indicate that mistletoe infection plays an important role in shaping the woody plant spatial patterns of this savanna. In addition, given the distribution of mistletoes worldwide, these findings have important implications for spatial patterning and heterogeneity in many ecosystems. However, this study is a snapshot, given that both *V. karroo* and mistletoes are long-lived species, thus long-term studies are required to provide a more complete understanding of how mistletoe infection contributes towards the spatial patterning and overall ecosystem heterogeneity over longer periods. Perhaps the differences between plot 1 versus plots 2 and 3 are an indication of different successional stages. As such, it is possible that the larger mature trees in plot 1 underwent density-dependent thinning and had regularly spaced mature trees, as opposed to the tree density in plots 2 and 3, which may be going through density-dependent thinning and thus having more aggregated younger trees.

Funding

This research did not receive any specific grant from funding agencies in the public, commercial, or not-for-profit sectors.

CRediT authorship contribution statement

Justice Muvengwi: Methodology, Formal analysis, Conceptualization. **Tsitsi Sithandiwe Maponga:** Writing – original draft, Methodology, Investigation, Formal analysis, Conceptualization. **Hilton Ndagurwa:** Writing – review & editing, Supervision, Conceptualization. **Ed Witkowski:** Writing – review & editing, Supervision, Conceptualization.

Declaration of Competing Interest

All authors declare that they do not have any competing interests.

Data availability

Data will be made available on request.

Acknowledgements

We thank the management of Matopos Research Station for allowing us to do research at the station. We are grateful to Melusi Sibanda, Sibongile Sibusisiwe Maponga, Moreblessings T. Tshuma, Farai Musiyandaka, Muziwandile Sibanda, Sihlangene Nali Moyo and Thembelani Bhebhe, for assisting with data collection.

Financial interests

All the authors declare they have no financial interests

Appendix A. Supporting information

Supplementary data associated with this article can be found in the online version at doi:10.1016/j.gecco.2024.e02931.

References

Arruda, R., Fadini, R.F., Carvalho, L.N., Del-Claro, K., Mourão, F.A., Jacobi, C.M., Teodoro, G.S., Berg, E.V.D., Caires, C.S., Dettke, G.A., 2012. Ecology of neotropical mistletoes: an important canopy-dwelling component of Brazilian ecosystems. Acta Bot. Bras. *26*, 264–274. https://doi.org/10.1590/S0102-33062012000200003.

Aukema, J.E., 2004. Distribution and dispersal of desert mistletoe is scale-dependent, hierarchically nested. Ecography *27* (2), 137–144. https://doi.org/10.1111/j.0906-7590.2004.03640.x.

Baddeley, A., Rubak, E., Turner, R., 2015. Spat. Point Pattern.: Methodol. Appl. R. CRC Press.

Baddeley, A., Diggle, P.J., Hardegen, A., Lawrence, T., Milne, R.K., Nair, G., 2014. On tests of spatial pattern based on simulation envelopes. Ecol. Monogr. *84* (3), 477–489. https://doi.org/10.1890/13-2042.1.

Barot, S., Gignoux, J., Menaut, J.C., 1999. Demography of a savanna palm tree: predictions from comprehensive spatial pattern analyses. Ecology *80* (6), 1987–2005. https://doi.org/10.1890/0012-9658(1999)080[1987:DOASPT]2.0.CO;2.

Belsky, A.J., 1994. Influences of trees on savanna productivity: tests of shade, nutrients, and tree-grass competition. Ecology *75* (4), 922–932. https://doi.org/10.2307/1939416.

Bilgili, E., Coskuner, K.A., Ozturk, M., 2020. Leaf area - sapwood area relationship in Scots pine (Pinus sylvestris L.) under mistletoe (Viscum album ssp. austriacum) infection. Dendrobiology 84, 1–11. https://doi.org/10.12657/denbio.084.001.

Bilgili, E., Ozturk, M., Coskuner, K.A., Baysal, I., Serdar, B., Yavuz, H., Usta, Y., 2018. Quantifying the effect of pine mistletoe on the growth of Scots pine. For. Pathol. 48 (4), 1–9. https://doi.org/10.1111/efp.12435.

Bilgili, E., Coskuner, K.A., Baysal, I., Ozturk, M., Usta, Y., Eroglu, M., Norton, D., 2020a. The distribution of pine mistletoe (Viscum album ssp. austriacum) in Scots pine (Pinus sylvestris) forests: from stand to tree level. Scand. J. For. Res. 35 (1-2), 20–28. https://doi.org/10.1080/02827581.2020.1729402.

Bowie, M., Ward, D., 2004. Water and nutrient status of the mistletoe *Plicosepalus acaciae* parasitic on isolated Negev desert populations of *Acacia raddiana* differing in level of mortality. J. Arid Environ. 56, 487–508. https://doi.org/10.1016/S0140-1963(03)00067-3.

Cheng, X., Han, H., Kang, F., Song, Y., Liu, K., 2014. Point pattern analysis of different life stages of *Quercus liaotungensis* in Lingkong Mountain, Shanxi Province, China. J. Plant Interact. *9* (1), 233–240. https://doi.org/10.1080/17429145.2013.818167.

Chirara, C., Frost, P.G.H., Gwarazimba, V.E.E., 1998. Grass defoliation affecting survival and growth of seedlings of *Acacia karroo*, an encroaching species in southwestern Zimbabwe. Afr. J. Range Forage Sci. *15* (1-2), 41–47. https://doi.org/10.1080/10220119.1998.9647939.

Dale, M.R., 2000. Spatial pattern analysis in plant ecology. Cambridge University press.

Daryaei, M.G., Moghadam, E.S., 2012. Effects of mistletoe (Viscum album L.) on leaves and nutrients content of some host trees in hyrcanian forests (Iran). Int. J. Agric. Res. Rev 2 (3), 85–90.

Dean, W.R.J., Midgley, J.J., Stock, W.D., 1994. The distribution of mistletoes in South Africa: patterns of species richness and host choice. J. Biogeogr. *21* (5), 503–510. https://doi.org/10.2307/2845654.

Dohn, J., Augustine, D.J., Hanan, N.P., Ratnam, J., Sankaran, M., 2017. Spatial vegetation patterns and neighborhood competition among woody plants in an East African savanna. Ecology *98* (2), 478–488. https://doi.org/10.1002/ecy.1659.

Dye, P.J. 1983. Prediction of variation in grass growth in a semi-arid induced grassland. PhD thesis, University of the Witwatersrand, Johannesburg, South Africa.

Dyer, C., 2014. New names for the African Acacia species in Vachellia and Senegalia. Southern Forests: a Journal of Forest Science 76 (4), iii. https://doi.org/10.2989/20702620.2014.980090.

Dzerefos, C.M., Witkowski, E.T.F., Shackleton, C.M., 2003. Host-preference and density of woodrose-forming mistletoes (Loranthaceae) on savanna vegetation, South Africa. Plant Ecol. 167, 163–177. https://doi.org/10.1023/A:1023991514968.

Flores, J., Jurado, E., 2003. Are nurse-protégé interactions more common among plants from arid environments? J. Veg. Sci. *14* (6), 911–916. https://doi.org/10.1111/j.1654-1103.2003.tb02225.x.

Fortin M.J., Dale M.R.T. (2005). Spatial Analysis: A Guide for Ecologists. Cambridge University Press, New York.

Getzin, S., Worbes, M., Wiegand, T., Wiegand, K., 2011. Size dominance regulates tree spacing more than competition within height classes in tropical Cameroon. J. Trop. Ecol. *27* (1), 93–102. https://doi.org/10.1017/S0266467410000453.

Getzin, S., Dean, C., He, F., Trofymow, J.A., Wiegand, K., Wiegand, T., 2006. Spatial patterns and competition of tree species in a Douglas-fir chronosequence on Vancouver Island. Ecography *29* (5), 671–682. https://doi.org/10.1111/j.2006.0906-7590.04675.x.

Kanz W.A. (1996). The effect of trees on their immediate environment. Honours dissertation. University of Natal, Pietermaritzburg.

Kavanagh, P.H., Burns, K.C., 2012. Mistletoe macroecology: spatial patterns in species diversity and host use across Australia. Biol. J. Linn. Soc. *106* (3), 459–468. https://doi.org/10.1111/j.1095-8312.2012.01890.x.

Kolodziejek, J., Kolodziejek, A., 2013. The Spatial Distribution of Pine Mistletoe Viscum album Ssp Austriacum (Wiesb.) Volmann in a Scots Pine (Pinus sylvestris L) Stand in Central Poland. Pol. J. Ecol. 61 (4), 705–714.

Maponga, T.S., 2021. Mistletoes as drivers of plant community structure and resource heterogeneity in semi-arid savanna ecosystems, Zimbabwe. PhD, University of the Witwatersrand, Johannesburg.

Maponga, T.S., Ndagurwa, H.G.T., Witkowski, E.T., 2021. Functional and species composition of understory plants varies with mistletoe-infection on *Vachellia karroo* trees in a semi-arid African savanna. Glob. Ecol. Conserv. *32*, e01897 https://doi.org/10.1016/j.gecco.2021.e01897.

Martínez, I., Wiegand, T., González-Taboada, F., Obeso, J.R., 2010. Spatial associations among tree species in a temperate forest community in North-western Spain. For. Ecol. Manag. *260* (4), 456–465. https://doi.org/10.1016/j.foreco.2010.04.039.

Mathiasen, R.L., Hawksworth, F.G., Edminster, C.B., 1990. Effects of dwarf mistletoe on growth and mortality of Douglas-fir in the Southwest. Gt. Basin Nat. 50 (2), 173–179. https://www.jstor.org/stable/41712589.

Mellado, A., Zamora, R., 2017. Parasites structuring ecological communities: the mistletoe footprint in Mediterranean pine forests. Funct. Ecol. *31* (11), 2167–2176. https://doi.org/10.1111/1365-2435.12907.

Mellado, A., Morillas, L., Gallardo, A., Zamora, R., 2016. Temporal dynamic of parasite-mediated linkages between the forest canopy and soil processes and the microbial community. N. Phytol. *211* (4), 1382–1392. https://doi.org/10.1111/nph.13984.

Meyer, K.M., Ward, D., Wiegand, K., Moustakas, A., 2008. Multi-proxy evidence for competition between savanna woody species. Perspect. Plant Ecol., Evol. Syst. *10* (1), 63–72. https://doi.org/10.1016/j.ppees.2007.09.002.

Moustakas, A., Wiegand, K., Getzin, S., Ward, D., Meyer, K.M., Guenther, M., Mueller, K.H., 2008. Spacing patterns of an Acacia tree in the Kalahari over a 61-year period: How clumped becomes regular and vice versa. Acta Oecologica *33* (3), 355–364. https://doi.org/10.1016/j.actao.2008.01.008.
Moyo, B., Dube, S., Moyo, C., Nesamvuni, E., 2011. Heavily stocked 5-paddock rotational grazing effect on cross-bred Afrikaner steer performance and herbaceous vegetation dynamics in a semi-arid veld of Zimbabwe. Afr. J. Agric. Res. *6* (10), 2166–2174. https://doi.org/10.5897/AJAR.9000384.
Mupangwa, W., Twomlow, S., Walker, S., 2013. Cumulative effects of reduced tillage and mulching on soil properties under semi-arid conditions. J. Arid Environ. *91*, 45–52. https://doi.org/10.1016/j.jaridenv.2012.11.007.
Muvengwi, J., Ndagurwa, H.G.T., Nyenda, T., 2015. Enhanced soil nutrient concentrations beneath-canopy of savanna trees infected by mistletoes in a southern African savanna. J. Arid Environ. 116, 25–28. https://doi.org/10.1016/j.jaridenv.2015.01.017.
Muvengwi, J., Davies, A.B., Parrini, F., Witkowski, E.T., 2018a. Geology drives the spatial patterning and structure of termite mounds in an African savanna. Ecosphere 9 (3), e02148. https://doi.org/10.1002/ecs2.2148.
Muvengwi, J., Mbiba, M., Chikumbindi, J., Ndagurwa, H.G., Mureva, A., 2018b. Population structure and spatial point-pattern analysis of a mono stand of *Acacia polyacantha* along a catena in a savanna ecosystem. For. Ecol. Manag. 409, 499–508. https://doi.org/10.1016/j.foreco.2017.11.056.
Muvengwi, J., Ndagurwa, H.G., Mbiba, M., Witkowski, E.T.F., 2020. Structure and spatial interactions of savanna trees along a local stress gradient in a semi-arid environment. Folia Geobot. *55*, 195–209. https://doi.org/10.1007/s12224-020-09374-4.
Muvengwi, J., Ndagurwa, H.G., Nyenda, T., Mwembe, R., Mbiba, M., 2017. Spatial pattern analysis of encroaching tree species (*Vachellia karroo* and *Vachellia nilotica*) after fire suppression in a semi-arid savanna. J. Trop. Ecol. *33* (6), 411–414. https://doi.org/10.1017/S0266467417000384.
Ndagurwa, H.G., Dube, J.S., Mlambo, D., 2013. The influence of mistletoes on nitrogen cycling in a semi-arid savanna, south-west Zimbabwe. J. Trop. Ecol. *29* (2), 147–159. https://doi.org/10.1017/S0266467413000096.
Ndagurwa, H.G., Dube, J.S., Mlambo, D., 2014. The influence of mistletoes on nutrient cycling in a semi-arid savanna, southwest Zimbabwe. Plant Ecol. *215*, 15–26. https://doi.org/10.1007/s11258-013-0275-x.
Ndagurwa, H.G., Dube, J.S., Mlambo, D., 2015. Decomposition and nutrient release patterns of mistletoe litters in a semi-arid savanna, southwest Zimbabwe. Austral Ecol. *40* (2), 178–185. https://doi.org/10.1111/aec.12191.
Ndagurwa, H.G., Maponga, T.S., Muvengwi, J., 2020. Mistletoe litter accelerates the decomposition of recalcitrant host litter in a semi-arid savanna, south-west Zimbabwe. Austral Ecol. *45* (8), 1080–1092. https://doi.org/10.1111/aec.12935.
Ndagurwa, H.G., Mundy, P.J., Dube, J.S., Mlambo, D., 2012. Patterns of mistletoe infection in four *Acacia* species in a semi-arid southern African savanna. J. Trop. Ecol. 28 (5), 523–526. https://doi.org/10.1017/s0266467412000387.
Ndagurwa, H.G., Dube, J.S., Mlambo, D., Mawanza, M., 2014. The influence of mistletoes on the litter-layer arthropod abundance and diversity in a semi-arid savanna, Southwest Zimbabwe. Plant Soil *383*, 291–299. https://doi.org/10.1007/s11104-014-2176-8.
Ndagurwa, H.G., Ndarevani, P., Muvengwi, J., Maponga, T.S., 2016. Mistletoes via input of nutrient-rich litter increases nutrient supply and enhance plant species composition and growth in a semi-arid savanna, southwest Zimbabwe. Plant Ecol. *217*, 1095–1104. https://doi.org/10.1007/s11258-016-0635-4.
Ndagurwa, H.G., Maponga, T.S., Dube, B., Nzuma, T.M., Muvengwi, J., 2018. Termitaria vs. mistletoe: effects on soil properties and plant structure in a semi-arid savanna. Acta Oecologica *91*, 35–42. https://doi.org/10.1016/j.actao.2018.06.002.
Ndagurwa, H.G.T., Dube, J.S., 2013. Evaluation of potential and effective rumen digestion of mistletoe species and woody species browsed by goats in a semi-arid savanna, southwest Zimbabwe. Anim. Feed Sci. Technol. *186* (1-2), 106–111. https://doi.org/10.1111/aec.12191.
O'Connor, T.G., 1995. *Acacia karroo* invasion of grassland: environmental and biotic effects influencing seedling emergence and establishment. Oecologia 103 (2), 214–223. ⟨https://www.jstor.org/stable/4221023⟩.
Okubamichael, D.Y., Griffiths, M.E., Ward, D., 2011. Host specificity, nutrient and water dynamics of the mistletoe *Viscum rotundifolium* and its potential host species in the Kalahari of South Africa. J. Arid Environ. 75, 898–902. https://doi.org/10.1016/j.jaridenv.2011.04.026.
Okubamichael, D.Y., Griffiths, M.E., Ward, D., 2014. Reciprocal transplant experiment suggests host specificity of the mistletoe *Agelanthus natalitius* in South Africa. J. Trop. Ecol. 30, 153–163. https://doi.org/10.1017/S0266467413000801.
Okubamichael, D.Y., Rasheed, M.Z., Griffiths, M.E., Ward, D., 2011b. Avian consumption and seed germination of the hemiparasitic mistletoe *Agelanthus natalitius* (Loranthaceae). J. Ornithol. 152, 643–649. https://doi.org/10.1007/s10336-010-0624-7.
Overton, J.M., 1996. Spatial autocorrelation and dispersal in mistletoes: field and simulation results. Vegetatio *125*, 83–98. https://doi.org/10.1007/BF00045207.
Ovincent, V., Thomas, R.G. and Staples, R.R., 1960. An agricultural survey of Southern Rhodesia. Part 1. Agro-ecological survey. An agricultural survey of Southern Rhodesia. Part 1. Agro-ecological survey.
Ozturk, M., Coskuner, K.A., Serdar, B., Atar, F., Bilgili, E., 2022. Impact of white mistletoe (Viscum album ssp. abietis) infection severity on morphology, anatomy and photosynthetic pigment content of the needles of cilicican fir (Abies cilicica). Flora 294, 152135. https://doi.org/10.1016/j.flora.2022.152135.
Pablo, R., Gusman, E., 2017. Ecology and Space: an Approach from Point Patterns. Res. Rev.: J. Bot. Sci. 6 (3), 71–74.
Pennings, S.C., Callaway, R.M., 1996. Impact of a parasitic plant on the structure and dynamics of salt marsh vegetation. Ecology 77 (5), 1410–1419. https://doi.org/10.2307/2265538.
Phillips, D.L., MacMahon, J.A., 1981. Competition and spacing patterns in desert shrubs. J. Ecol. 97–115. https://doi.org/10.2307/2259818.
Pillay, T., Ward, D., 2012. Spatial pattern analysis and competition between *Acacia karroo* trees in humid savannas. Plant Ecol. *213*, 1609–1619. https://doi.org/10.1007/s11258-012-0115-4.
Pinto, M.M., 2005. Studies of the population ecology of the mistletoe *Phoradendron anceps* (Viscaceae) and its host *Pisonia albida* (Nyctaginaceae) in the guánica forest reserve, Puerto Rico. University of Puerto Rico, Mayaguez (Puerto Rico.
Press, M.C., Phoenix, G.K., 2005. Impacts of parasitic plants on natural communities. N. Phytol. *166* (3), 737–751. https://doi.org/10.1111/j.1469-8137.2005.01358.x.
Preston, A., An, M., Watson, D., 2010. Chemical profile differences in endemic parasitic weeds: a study of host-parasite chemical profiles in select mistletoe and eucalypt species. In: Australasian Weeds Conference (AWC). Zealand Plant Protection Society (Inc, New, pp. 373–374).
R Core Team (2020). R: A language and environment for statistical computing. R Foundation for Statistical Computing, Vienna, Austria. URL https://www.R-project.org/.
Rayburn, A.P., Monaco, T.A., 2011. Linking plant spatial patterns and ecological processes in grazed Great Basin plant communities. Rangel. Ecol. Manag. *64* (3), 276–282. https://doi.org/10.2111/REM-D-10-00130.1.
Roxburgh, L., Nicolson, S.W., 2005. Patterns of host use in two African mistletoes: the importance of mistletoe-host compatibility and avian disperser behaviour. Funct. Ecol. *19* (5), 865–873. ⟨https://www.jstor.org/stable/3599349⟩.
Roxburgh, L., Nicolson, S.W., 2008. Differential dispersal and survival of an African mistletoe: does host size matter? Plant Ecol. *195*, 21–31. https://doi.org/10.1007/s11258-007-9295-8.
Sala, A., Carey, E.V., Callaway, R.M., 2001. Dwarf mistletoe affects whole-tree water relations of Douglas fir and western larch primarily through changes in leaf to sapwood ratios. Oecologia 126, 42–52. https://doi.org/10.1007/s004420000.
Sayad, E., Boshkar, E., Gholami, S., 2017. Different role of host and habitat features in determining spatial distribution of mistletoe infection. For. Ecol. Manag. *384*, 323–330. https://doi.org/10.1016/j.foreco.2016.11.012.
Schleicher, J., Meyer, K.M., Wiegand, K., Schurr, F.M., Ward, D., 2011. Disentangling facilitation and seed dispersal from environmental heterogeneity as mechanisms generating associations between savanna plants. J. Veg. Sci. *22* (6), 1038–1048. https://doi.org/10.1111/j.1654-1103.2011.01310.x.
Spasojevic, M.J., Suding, K.N., 2011. Contrasting effects of hemiparasites on ecosystem processes: can positive litter effects offset the negative effects of parasitism? Oecologia 165, 193–200. https://www.jstor.org/stable/41500621.
Svátek, M., Rejžek, M., Kvasnica, J., Řepka, R., Matula, R., 2018. Frequent fires control tree spatial pattern, mortality and regeneration in Argentine open woodlands. For. Ecol. Manag. *408*, 129–136. https://doi.org/10.1016/j.foreco.2017.10.048.
Tamjidi, J., Lutz, J.A., 2020. The post-fire assembly processes of tree communities based on spatial analysis of a Sierra Nevada mixed-conifer forest. Fire *3* (4), 72. https://doi.org/10.3390/fire3040072.

Velázquez, E., De la Cruz, M., Gomez-Sal, A., 2014. Changes in spatial point patterns of pioneer woody plants across a large tropical landslide. Acta Oecologica 61, 9–18. https://doi.org/10.1016/j.actao.2014.09.001.
Walters, M., Milton, S.J., 2003. The production, storage and viability of seeds of *Acacia karroo* and *A. nilotica* in a grassy savanna in KwaZulu-Natal, South Africa. Afr. J. Ecol. *41* (3), 211–217. https://doi.org/10.1046/j.1365-2028.2003.00433.x.
Ward, D., Shrestha, M.K., Musli, I., 2006. Are invasive mistletoes killing *Ziziphus spina-christi*? Isr. J. Plant Sci. *54*, 113–117. https://doi.org/10.1560/IJPS_54_2_113.
Ward, D., Pillay, T., Mbongwa, S., Kirkman, K., 2022. Spatial analysis reveals facilitation in young clonal trees and competition in older trees during re-invasion of encroaching trees in an African savanna. Plant Ecol. *223*, 1167–1180. https://doi.org/10.1007/s11258-022-01263-4.
Wiegand, T., Moloney, K., 2004. Rings, circles, and null-models for point pattern analysis in ecology. Oikos 104 (2), 209–229. https://doi.org/10.1111/j.0030-1299.2004.12497.x.
Wiegand, T. and Moloney, K.A., 2013. Handbook of spatial point-pattern analysis in ecology. CRC press.
Wilson, T.B., Witkowski, E.T.F., 1998. Water requirements for germination and early seedling establishment in four African savanna woody plant species. J. Arid Environ. *38* (4), 541–550. https://doi.org/10.1006/jare.1998.0362.
Witkowski, E.T.F., Garner, R.D., 2000. Spatial distribution of soil seed banks of three African savanna woody species at two contrasting sites. Plant Ecol. *149*, 91–106. https://doi.org/10.1023/A:1009850706843.

Further reading

Csurhes, S., 2016. Invasive plant risk assessment. *Bitou bush*. Dep. Agric. Fish. Biosecurity Qld.
Walters, M., Milton, S.J., Somers, M.J., Midgley, J.J., 2005. Post-dispersal fate of *Acacia* seeds in an African savanna. South Afr. J. Wildl. Res. 35 (2), 191–199. https://hdl.handle.net/10520/EJC117214.